Inorg. Chem. **2005**, *44*, 6445–6455

Laser Photolysis Studies of the Reaction of Chromium(III) Octaethylporphyrin Complex with Triphenylphosphine and Triphenylphosphine Oxide

Masahiko Inamo,*,† Nao Matsubara,† Kiyohiko Nakajima,† Tsutomu S. Iwayama,‡ Hiroshi Okimi,§ and Mikio Hoshino*,§

Departments of Chemistry and Physics, Aichi University of Education, Kariya, Aichi 448-8542, Japan, and The Institute of Physical and Chemical Research, Wako, Saitama 351-0189, Japan

Received March 25, 2005

The photoreaction of the chromium(III) octaethylpoprhyrin complex, [Cr(OEP)(Cl)(L)] (L = H_2O, Py, $OPPh_3$), in dichloromethane was studied using laser flash photolysis technique. Laser irradiation causes the generation of a coordinately unsaturated intermediate [Cr(OEP)(Cl)], which reacts with ligands in solution to give the parent complex, [Cr(OEP)(Cl)(L)], or a transient species, [Cr(OEP)(Cl)(H_2O)], when L = Py or $OPPh_3$. Once produced [Cr(OEP)(Cl)(H_2O)] eventually exchanges the axial H_2O ligand with L to regenerate [Cr(OEP)(Cl)(L)]. The kinetics of the axial ligand substitution reaction was followed spectrophotometrically, and the ligand-concentration dependence of the ligand exchange rate revealed that the reaction occurs via a limited dissociative mechanism. The photoreaction of [Cr(OEP)(Cl)($OPPh_3$)] containing excess PPh_3 in the bulk solution leads to the unfavorable coordination of the PPh_3 molecule to the chromium ion to give a transient complex, [Cr(OEP)(Cl)(PPh_3)]. The dynamic and thermodynamic properties of [Cr(OEP)(Cl)(PPh_3)] in solution are discussed on the basis of the kinetic parameters of the dissociation and association reactions of the PPh_3 ligand together with the steric aspect of the molecular structure of the related complexes.

Introduction

Chromium porphyrins have been extensively studied as catalysts for various organic syntheses such as the epoxide carbonylation reaction,[1] polycarbonate formation,[2,3] and polyene polymer epoxidation.[4] In the former two cases, the chromium(III) porphyrin complex acts as a Lewis acid in the catalytic reactions, and the nature of the axial coordination site of the central chromium atom related to such catalytic activity of the complex has been extensively investigated to elucidate the mechanism of the catalytic reactions. It has been well-recognized that the axial position of the metalloporphyrins is labilized more than several orders of magnitude in rate as compared with the complex having nonmacrocyclic ligands, and this labilizing effect due to the porphyrin ligation plays an important role in the catalytic activity of the chromium(III) porphyrin complexes.[5−17] To elucidate the mechanism of this labilizing effect, the dynam-

* To whom correspondence should be addressed. E-mail: minamo@auecc.aichi-edu.ac.jp.
† Department of Chemistry, Aichi University of Education.
‡ Department of Physics, Aichi University of Education.
§ The Institute of Physical and Chemical Research.

(1) Schmidt, J. A. R.; Mahadevan, V.; Getzier, Y. D. Y. L.; Coates, G. W. *Org. Lett.* **2004**, *6*, 373−376.
(2) Stamp, L. M.; Mang, S. A.; Holmes, A. B.; Knights, K. A.; de Miguel, Y. R.; McConvey, I. F. *Chem. Commun.* **2001**, 2502−2503.
(3) Mang, S.; Cooper, A. I.; Colclough, M. E.; Chauhan, N.; Holmes, A. B. *Macromolecules* **2000**, *33*, 303−308.
(4) Davaras, E. M.; Diaper, R.; Dervissi, A.; Tornaritis, M. J.; Coutsolelos, A. G. *J. Porphyrins Phthalocyanines* **1998**, *2*, 53−60.
(5) Fleischer, E. B.; Krishnamurthy, M. *J. Am. Chem. Soc.* **1971**, *93*, 3784−3786.
(6) Fleischer, E. B.; Krishnamurthy, M. *J. Coord. Chem.* **1972**, *2*, 89−100.
(7) Krishnamurthy, M. *Inorg. Chim. Acta* **1978**, *26*, 137−144.
(8) Ashley, K. R.; Leipoldt, J. G.; Joshi, V. K. *Inorg. Chem.* **1980**, *19*, 1608−1612.
(9) Leipoldt, J. G.; Basson, S. S.; Rabie, D. R. *J. Inorg. Nucl. Chem.* **1981**, *43*, 3239−3244.
(10) O'Brien P.; Sweigart, D. A. *Inorg. Chem.* **1982**, *21*, 2094−2095.
(11) Leipoldt, J. G.; van Eldik, R.; Kelm, H. *Inorg. Chem.* **1983**, *22*, 4146−4149.
(12) Leipoldt, J. G.; Meyer, H. *Polyhedron* **1987**, *6*, 1361−1364.
(13) Ashley, K. R.; Kuo, J. *Inorg. Chem.* **1988**, *27*, 3556−3561.
(14) Ashley, K. R.; Trent, I. *Inorg. Chim. Acta* **1989**, *163*, 159−166.
(15) Inamo, M.; Sumi, T.; Nakagawa, N.; Funahashi, S.; Tanaka, M. *Inorg. Chem.* **1989**, *28*, 2688−2691.
(16) Inamo, M.; Sugiura, S.; Fukuyama, H.; Funahashi, S. *Bull. Chem. Soc. Jpn.* **1994**, *67*, 1848−1854.
(17) Inamo, M.; Nakajima, K. *Bull. Chem. Soc. Jpn.* **1998**, *71*, 883−891.

10.1021/ic0504487 CCC: $30.25
Published on Web 08/02/2005

ics of the axial ligand substitution reaction of the chromium(III) porphyrin complexes has been studied using various techniques, including conventional spectrophotometric method and laser flash photolysis. It has been revealed that in many cases the substitution reaction proceed via a limiting dissociative mechanism in which a coordinately unsaturated intermediate species is included. The high reactivity coupled with the facile ligand substitution reaction at the axial coordination site of the porphyrin complexes is of fundamental interest for the information they provide on the chemistry of porphyrin complexes in solution.

We have been interested in the dynamics of the photoinduced reaction of the chromium(III) porphyrin complexes as well as the axial ligand substitution, and laser flash photolysis has been employed to investigate the mechanisms of various photophysical and photochemical processes, including photoinduced axial ligand dissociation and recombination reactions.[18−23] The reactivity of the metalloporphyrins in the ground and excited states are affected by various factors, i.e., the molecular structure of the complex, the electronic structure, and the axial ligation.[24] In the present study, in a continuing effort to develop our understanding of the chromium porphyrin chemistry, we investigated the reaction of the chromium(III) complex of 2,3,7,8,12,13,17,-18-octaethylporphyrin with triphenylphosphine in dichloromethane with respect to the effect of the steric bulk of the axial ligand on the dynamics of the ligand substitution reaction using a nanosecond laser flash photolysis technique. Studies on the dynamics of the reactions of the triphenylphosphine complex in solution may provide some insight into the effect of steric bulk around the coordinating phosphorus atom on the reactivity of the porphyrin complex toward the axial ligand. The mechanism of the steric effect of the bulky ligand on the reaction dynamics will be discussed on the basis of the kinetics of the photoinduced reactions.

Experimental Section

General Information. Aquachloro(2,3,7,8,12,13,17,18-octaethylporphyrinato)chromium(III), [Cr(OEP)(Cl)(H_2O)] (**1**), was prepared and purified according to the synthetic procedure for the chromium(III) 5,10,15,20-tetraphenylporphyrin complex, [Cr(TPP)-(Cl)(H_2O)].[18,25] Pyridine (Py, Wako Pure Chemicals) was dried over solid potassium hydroxide and then distilled. Triphenylphosphine (PPh_3, Wako) was purified by vacuum sublimation. Triphenylphosphine oxide ($OPPh_3$, Wako) was recrystallized from a mixture of ethanol and diethyl ether. Dichloromethane (spectral grade, Nakalai Tesque) stabilized with 10 ppm 2-methyl-2-butene was used without further purification. Anal. Calcd for **1** ($C_{36}H_{46}ClCrN_4O\cdot0.3H_2O$): C, 67.18; H, 7.30; N, 8.70; Cl, 5.51. Found: 67.17; H, 7.32; N, 8.43; Cl, 5.67. Dark violet crystals of [Cr(TPP)(Cl)($OPPh_3$)] for the X-ray crystallography were obtained by slow evaporation of the solvent from a 1,2-dichloroethane−toluene solution. The precipitated purple crystalline product was filtered and dried. Anal. Calcd for $C_{62}H_{43}N_4OPClCr$: C, 76.11; H, 4.43; N, 5.73. Found: C, 76.09; H, 4.62; N, 5.79.

Absorption spectra were recorded on a Hitachi U-3000 spectrophotometer. Laser photolysis studies were carried out with a Nd:YAG laser (Surelite, Continuum) equipped with second (532 nm) and third (355 nm) harmonic generators. The duration of the laser pulse was 6 ns. The transient spectra were measured by an intensified charge-coupled device detector (DH 520-18F-01, Andor Technology). The decay of the transient absorption was monitored by a detection system (TSP-601, Unisoku, Japan). The intensity of the analyzing light beam from a xenon lamp (L2195, Hamamatsu Photonics) passed through a sample cell was measured by a photomultiplier (R2949, Hamamatsu Photonics) attached to the exit of a monochromator. The kinetics of the axial substitution reaction were studied using a stopped-flow spectrophotometer (Unisoku). The temperature of the solutions was controlled to within ±0.1 °C using a thermostated circulating water bath. The concentration of the chromium(III) porphyrin complex in dichloromethane was less than 1.0×10^{-5} mol kg^{-1}; and that of the axial ligand, more than 1.0×10^{-4} mol kg^{-1}. The concentration of water in the dichloromethane solution was determined by a Karl Fischer titrator (CA-06, Mitsubishi Chemicals).

The kinetics of the bleaching and those of the positive transients were the same for all photoinduced reactions. The experimental pseudo-first-order rate constant k_{obsd} was obtained from the nonlinear least-squares analysis of the absorbance−time traces observed for the laser flash photolysis and stopped-flow experiments. The reaction curves were averaged several times on the digital oscilloscope. The estimated standard deviation of k_{obsd} was less than ±3%.

X-ray Crystallography. A prismatic single crystal ($0.18 \times 0.24 \times 0.50$ mm) of [Cr(TPP)(Cl)($OPPh_3$)] was glued onto a glass fiber and coated with epoxy resin to avoid intensity changes during the data collection. After removal from the mother liquor, the crystal deteriorated gradually due to loss of the crystallization solvent. Intensity data were collected on a Rigaku RAXIS−RAPID diffractometer with graphite-monochromated Mo Kα radiation (λ = 0.710 69 Å) at room temperature. The data were processed by the PROCESS-AUTO program package. A total of 23 096 reflections were collected to a maximum 2θ value of 55°, 12 999 of which were independent (R_{int} = 0.018). A set of 7522 reflections ($I > 2\sigma(I)$) was used for the structure determination and refinement. A numerical absorption correction using NUMABS[26] was applied. The structure was solved by direct methods (SIR92),[27] expanded using Fourier techniques (DIRDIF94),[28] and refined by full-matrix least-squares based on F with anisotropic displacement parameters for non-hydrogen atoms except for those of toluene and 1,2-dichloroethane. Hydrogen atoms were placed at idealized positions and included in the refinement with fixed isotropic thermal

(18) Inamo, M.; Hoshino, M.; Nakajima, K.; Aizawa, S.; Funahashi, S. *Bull. Chem. Soc. Jpn.* **1995**, *68*, 2293−2303.
(19) Hoshino, M.; Tezuka, N.; Inamo, M. *J. Phys. Chem.* **1996**, *100*, 627−632.
(20) Hoshino, M.; Nagamori, T.; Seki, H.; Chihara, T.; Tase, T.; Wakatsuki, Y.; Inamo, M. *J. Phys. Chem. A* **1998**, *102*, 1297−1303.
(21) Inamo, M.; Hoshino, M. *Photochem. Photobiol.* **1999**, *70*, 596−601.
(22) Inamo, M.; Nakaba, H.; Nakajima, K.; Hoshino, M. *Inorg. Chem.* **2000**, *39*, 4417−4423.
(23) Inamo, M.; Eba, K.; Nakano, K.; Itoh, N.; Hoshino, M. *Inorg. Chem.* **2003**, *42*, 6095−6105.
(24) Gouterman, M. In *The Porphyrins*; Dolphin, D., Ed.; Academic Press: New York, 1978; Vol. III, Chapter 1.
(25) Summerville, D. A.; Jones, R. D.; Hoffman, B. M.; Basolo, F. *J. Am. Chem. Soc.* **1977**, *99*, 8195−8202.
(26) Higashi, T. Program for Absorption Correction, Rigaku Corp., Tokyo, Japan, 1999.
(27) Altomare, A.; Cascarano, G.; Giacovazzo, C.; Guagliardi, A.; Burla, M. C.; Polidori, G.; Camalli, M. *J. Appl. Crystallogr.* **1994**, *27*, 435.
(28) Beurskens, P. T., Admiraal, G., Beurskens, G., Bosman, W. P., de Gelder, R., Israel, R., Smits, J. M. M. The DIRDIF-94 Program System, Technical Report of the Crystallography Laboratory, University of Nijmegen, The Netherlands, 1994.

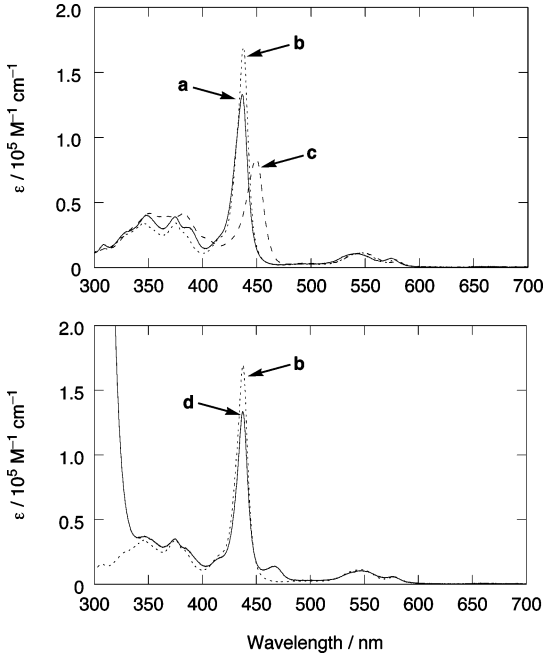

Figure 1. UV−visible absorption spectra of the dichloromethane solution of the Cr(III)−OEP complex. [Cr(OEP)(Cl)(H_2O)] (a), [Cr(OEP)(Cl)($OPPh_3$)] (b), [Cr(OEP)(Cl)(Py)] (c), and the solution containing the Cr(III)−OEP complex and PPh_3 (d).

parameters. All calculations were performed using the teXsan crystallographic software package of Molecular Structure Corp.[29] The relatively high *R*-factor value is due to the poor crystallinity. The atoms of toluene and 1,2-dichloroethane were highly disordered. The toluene molecule was found at two disordered positions. The Cl(2), Cl(3), C(68), and C(69) atoms of 1,2-dichloroethane were included in the final stages of the refinements with fixed parameters.

Results

UV−Visible Absorption Spectra of [Cr(OEP)(Cl)(L)] (L = H_2O, Py, $OPPh_3$, and PPh_3). It has been demonstrated that the chromium(III) porphyrin complex exists as [Cr(porphyrin)(Cl)(H_2O)] in a dichloromethane solution which contains a small amount of water.[22] The axial Cl ligand does not dissociate in a solvent with low dielectric constant such as dichloromethane.[25] The axial H_2O ligand, on the other hand, can be easily replaced with an external ligand such as Py and $OPPh_3$, as evidenced by the UV−visible absorption spectra shown in Figure 1. The change in the absorption spectrum upon introducing the ligand, L (L = $OPPh_3$ or Py), into the solution of [Cr(OEP)(Cl)(H_2O)] can be explained by the substitution reaction of the axial H_2O ligand to give [Cr(OEP)(Cl)(L)]. Meanwhile, the absorption spectrum of a solution that contains the Cr(III)−OEP complex and PPh_3 is very similar to that of [Cr(OEP)(Cl)($OPPh_3$)] with a slight difference around the Soret band, as shown in Figure 1. The intensity of the Soret band of the Cr(III)−OEP solution containing PPh_3 is slightly lower than that of [Cr(OEP)(Cl)($OPPh_3$)], and an additional weak absorption band appears at the lower energy region of the Soret band. We found that

(29) Crystal Structure Analysis Package, Molecular Structure Corp., 1985 and 1999.

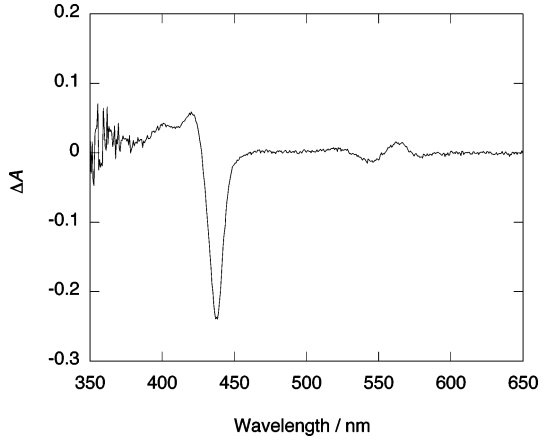

Figure 2. Transient spectra observed for the dichloromethane solution of [Cr(OEP)(Cl)(H_2O)] in the presence of 2.54×10^{-3} mol kg^{-1} H_2O. The spectra were taken at 20 ns after a 355 nm laser irradiation.

the reproducibility of the intensity of this weak band was poor and that its intensity strongly depends on the purity of PPh_3. Spectrum d in Figure 1 is observed when carefully purified PPh_3 is used. However, this spectrum is almost identical to that of [Cr(OEP)(Cl)($OPPh_3$)] observed with the use of commercially available PPh_3. These observations suggest that a trace amount of $OPPh_3$ may be contained in the solid PPh_3 as an impurity even if it is purified with meticulous care. Probably, $OPPh_3$ may preferentially coordinate to the chromium atom due to the smaller steric hindrance around the coordinating oxygen atom of $OPPh_3$ than the phosphorus atom in PPh_3. The small absorption band observed in the lower energy region of the Soret band of [Cr(OEP)(Cl)($OPPh_3$)], therefore, can be attributed to the Soret band of [Cr(OEP)(Cl)(PPh_3)], which will also be indicated by the transient absorption spectrum as mentioned later.

Photoreaction of [Cr(OEP)(Cl)(H_2O)] in Dichloromethane. The transient absorption difference spectrum observed after the laser irradiation of the dichloromethane solution of [Cr(OEP)(Cl)(H_2O)] is shown in Figure 2. The transient spectrum does not show the typical porphyrin triplet-state band around 500 nm.[19] The transient spectrum decays according to first-order kinetics without the formation of any permanent photoproducts. Dependence of the pseudo-first-order rate constants, k_{obsd}, on the concentration of H_2O contained in the dichloromethane solution is shown in Figure S1 (Supporting Information). We thus attribute the observed transient spectrum (Figure 2) to that of [Cr(OEP)(Cl)]. This is consistent with a similar finding for **1** in toluene.[23] Therefore, the photoinduced reaction can be expressed by

$$[\mathrm{Cr(OEP)(Cl)(H_2O)}] \xrightarrow{h\nu} [\mathrm{Cr(OEP)(Cl)}] + \mathrm{H_2O} \quad (1)$$

$$[\mathrm{Cr(OEP)(Cl)}] + \mathrm{H_2O} \underset{k_{-\mathrm{H_2O}}}{\overset{k_{\mathrm{H_2O}}}{\rightleftharpoons}} [\mathrm{Cr(OEP)(Cl)(H_2O)}] \quad (2)$$

Thus, k_{obsd} is given by

$$k_{\mathrm{obsd}} = k_{\mathrm{H_2O}}[\mathrm{H_2O}] + k_{-\mathrm{H_2O}} \quad (3)$$

where k_{H_2O} and k_{-H_2O} represent the second-order rate constant

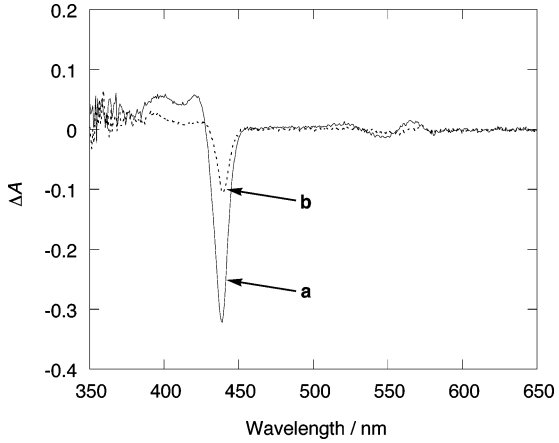

Figure 3. Transient spectra observed for the dichloromethane solution of [Cr(OEP)(Cl)($OPPh_3$)] in the presence of 1.90×10^{-3} mol kg^{-1} $OPPh_3$ and 1.83×10^{-3} mol kg^{-1} H_2O. The spectra were taken at 20 ns (a) and 1 μs (b) after a 355 nm laser irradiation.

for the recombination reaction of the H_2O molecule with the photoinduced five-coordinate complex, [Cr(OEP)(Cl)], and the first-order rate constant for the dissociation of the axial H_2O ligand, respectively. Since the rate constants k_{H_2O} and k_{-H_2O} are also included in the rate law of the photoreaction of [Cr(OEP)(Cl)(L)], where L represents the axial ligand such as Py, and the kinetic analysis of the data shown in Figure S1 (Supporting Information) using eq 3 will be described in a later section.

Photoreaction of [Cr(OEP)(Cl)($OPPh_3$)] and [Cr(OEP)(Cl)(Py)] in Dichloromethane. The transient spectra observed after laser irradiation of the dichloromethane solution of [Cr(OEP)(Cl)($OPPh_3$)] containing an excess amount of $OPPh_3$ are shown in Figure 3. The decay of the transient spectrum was found to be biphasic. The faster step of the decay, which we call the "fast process", is completed within 10^{-6} s after the laser pulse, and a much slower process ("slow process") follows it. As in the case of the photoreaction of [Cr(OEP)(Cl)(H_2O)], the transient spectrum observed just after the laser irradiation for [Cr(OEP)(Cl)($OPPh_3$)] does not have a broad absorption band around 500 nm that is typical for the triplet excited state of the porphyrin complex, while a new absorption band that can be attributed to the five-coordinate [Cr(OEP)(Cl)] was observed around 430 nm. The second transient has the same spectrum as [Cr(OEP)(Cl)(H_2O)] as shown in Figure S2 (Supporting Information) and is attributed to this species. The five-coordinate complex should also react with $OPPh_3$ to give the initial complex. The decay of the first transient spectrum to the second one can thus be ascribed to the parallel reactions of [Cr(OEP)(Cl)] with $OPPh_3$ and H_2O in the bulk solution to yield [Cr(OEP)(Cl)($OPPh_3$)] or [Cr(OEP)(Cl)(H_2O)], respectively. One of the products of the fast process, [Cr(OEP)(Cl)(H_2O)], is a transient species, and it finally reverts to the initial complex. The slow process can thus be attributed to the axial substitution reaction of the H_2O ligand in [Cr(OEP)(Cl)(H_2O)] by the entering ligand $OPPh_3$. A similar photoreaction was observed for [Cr(OEP)(Cl)(Py)] in the present study.[30]

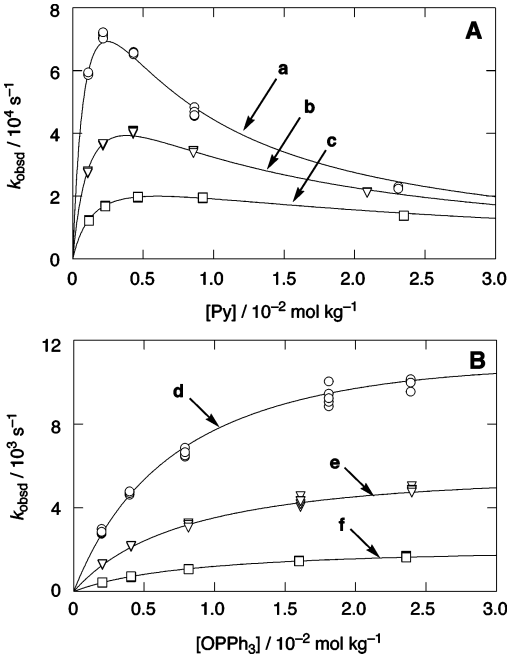

Figure 4. Plot of the pseudo-first-order rate constant k_{obsd} of the decay of [Cr(OEP)(Cl)(H_2O)] as a function of the concentration of pyridine (A) and of $OPPh_3$ (B) for the laser photolysis of [Cr(OEP)(Cl)(L)] (L represents pyridine and $OPPh_3$, respectively) in dichloromethane. [H_2O]/mol kg^{-1} = $(2.2-2.9) \times 10^{-3}$ (a), $(5.3-5.9) \times 10^{-3}$ (b), $(1.3-1.4) \times 10^{-2}$ (c), $(2.3-2.4) \times 10^{-3}$ (d), $(5.2-5.3) \times 10^{-3}$ (e), $(1.5-1.6) \times 10^{-2}$ (f). $T = 25.0$ °C.

Observed transient spectra for the reaction of [Cr(OEP)(Cl)(Py)] are shown in Figure S3 (Supporting Information).

The fast process consists of the parallel reversible reactions of 2 and 4:

$$[Cr(OEP)(Cl)] + OPPh_3 \underset{k_{-OPPh_3}}{\overset{k_{OPPh_3}}{\rightleftharpoons}} [Cr(OEP)(Cl)(OPPh_3)] \quad (4)$$

The absorbance−time traces can be expressed as the sum of two exponential functions. However, it is extremely difficult to determine rate constants of these reactions from reaction curves that seem to decay exponentially. Instead, each rate constant involved in these equations can be obtained from the kinetic analysis of the slow process.

In the slow process, the decay of the second transient spectrum to the original spectrum corresponds to the axial substitution reaction of H_2O in [Cr(OEP)(Cl)(H_2O)] by the entering ligand L (L = Py or $OPPh_3$) and obeys the first-order kinetics with respect to the porphyrin complex. k_{obsd} of the slow process was measured in the presence of an excess amount of the axial ligand L. The dependence of k_{obsd} on the ligand concentration in the bulk solution for the slow process of the photoreaction of [Cr(OEP)(Cl)(Py)] and [Cr(OEP)(Cl)($OPPh_3$)] is shown in Figure 4. In the case of [Cr(OEP)(Cl)(Py)], the reaction rate first increases with increases in the concentration of Py and then decreases at higher concentrations of Py. The rate constant also depends on the H_2O concentration in the bulk solution. These findings can be interpreted by the dissociative mechanism with a dead-

(30) In the previous study we described the photoreaction of [Cr(OEP)(Cl)(Py)] in toluene.[23] The solvent effect on the photoreaction mechanisms was revealed to be small for these two solvents.

Table 1. Kinetic and Thermodynamic Parameters[a] for the Axial Substitution Reaction of [Cr(OEP)(Cl)(L)] at $T = 25.0$ °C [b]

k_{-H_2O} (s^{-1})	4.17×10^5
$\Delta H_{-H_2O}^{\ddagger}$	57.2 ± 2.2
$\Delta S_{-H_2O}^{\ddagger}$	54.5 ± 7.2
k_{H_2O} (mol^{-1} kg s^{-1})	2.45×10^9
$\Delta H_{H_2O}^{\ddagger}$	7.2 ± 0.8
$\Delta S_{H_2O}^{\ddagger}$	-40.9 ± 2.7
k_{Py} (mol^{-1} kg s^{-1})	1.51×10^9
$\Delta H_{Py}^{\ddagger}$	6.7 ± 1.5
$\Delta S_{Py}^{\ddagger}$	-46.9 ± 5.0
$K_{(Py)}$ (mol^{-1} kg)	5.91×10^2
$\Delta H_{(Py)}^{\circ}$	-38.2 ± 1.9
$\Delta S_{(Py)}^{\circ}$	-74.9 ± 6.4
k_{OPPh_3} (mol^{-1} kg s^{-1})	2.33×10^7
$\Delta H_{OPPh_3}^{\ddagger}$	17.1 ± 1.1
$\Delta S_{OPPh_3}^{\ddagger}$	-46.4 ± 3.7
$K_{(OPPh_3)}$ (mol^{-1} kg)	1.13×10^2
$\Delta H_{(OPPh_3)}^{\circ}$	-24.8 ± 1.4
$\Delta S_{(OPPh_3)}^{\circ}$	-43.8 ± 5.0
k_{-PPh_3} (s^{-1})	1.61×10^5
$\Delta H_{-PPh_3}^{\ddagger}$	63.3 ± 1.6
$\Delta S_{-PPh_3}^{\ddagger}$	66.9 ± 5.4
k_{PPh_3} (mol^{-1} kg s^{-1})	5.53×10^8
$\Delta H_{PPh_3}^{\ddagger}$	12.6 ± 1.7
$\Delta S_{PPh_3}^{\ddagger}$	-35.4 ± 5.7

[a] ΔH, kJ mol^{-1}; ΔS, J mol^{-1} K^{-1}. [b] Values of the rate and equilibrium constants were calculated by using the determined $\Delta H^{\ddagger}$, $\Delta S^{\ddagger}$, ΔH°, and ΔS°.

end complex formation as a preequilibrium of the substitution reaction (eqs 5−7).

$$[Cr(OEP)(Cl)(H_2O)] + Py \overset{K_{(Py)}}{\rightleftharpoons} [Cr(OEP)(Cl)(HOH\text{---}Py)] \quad (5)$$

$$[Cr(OEP)(Cl)(H_2O)] \underset{k_{H_2O}}{\overset{k_{-H_2O}}{\rightleftharpoons}} [Cr(OEP)(Cl)] + H_2O \quad (6)$$

$$[Cr(OEP)(Cl)] + Py \xrightarrow{k_{Py}} [Cr(OEP)(Cl)(Py)] \quad (7)$$

The dead-end complex, [Cr(OEP)(Cl)(HOH···Py)], represents the complex in which the Py molecule binds to the hydrogen atom of the coordinating H_2O ligand in [Cr(OEP)(Cl)(H_2O)] by hydrogen bonding.[22] Because the formation of the hydrogen bond makes the O−H and Cr−O bonds weaker and stronger, respectively, in [Cr(OEP)(Cl)(HOH···Py)], the dissociation of the axial H_2O ligand should be suppressed. k_{obsd} is expressed by eq 8 by applying the steady-state approximation to the five-coordinate intermediate, [Cr(OEP)(Cl)].

$$k_{obsd} = k_{-H_2O}k_{Py}[Py]\,(k_{H_2O}[H_2O] + k_{Py}[Py])^{-1}\,(1 + K_{(Py)}[Py])^{-1} \quad (8)$$

The k_{-H_2O} and k_{H_2O} terms in this equation are the rate constants for the water dissociation and recombination reactions, respectively, and they are identical with those in eq 3. The kinetic results of the slow process of the photoreaction of [Cr(OEP)(Cl)(Py)] were simultaneously analyzed together with those of the photoreaction of [Cr(OEP)(Cl)(H_2O)] using a weighted-least-squares fitting calculation based on eqs 3 and 8. The kinetic and thermodynamic parameters obtained are listed in Table 1. The solid lines in Figures S1 (Supporting Information) and 4 were calculated using the kinetic parameters obtained.

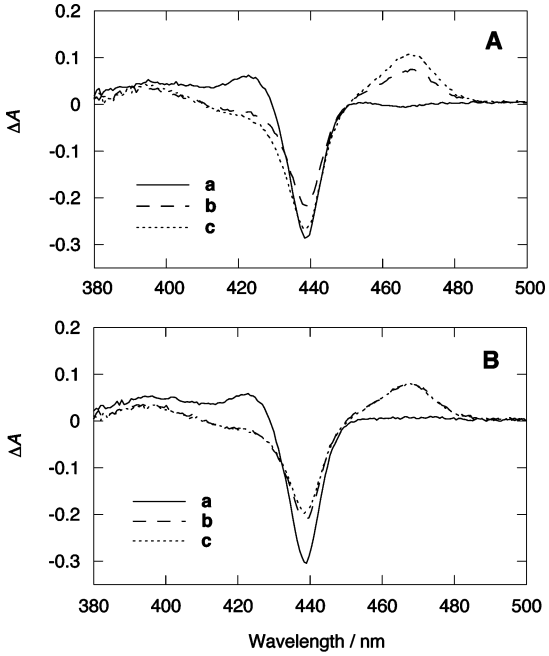

Figure 5. Transient spectra observed for the dichloromethane solution of [Cr(OEP)(Cl)($OPPh_3$)] in the presence of 1.90×10^{-3} mol kg^{-1} $OPPh_3$, 9.80×10^{-3} mol kg^{-1} PPh_3, and 1.45×10^{-3} mol kg^{-1} H_2O (A) and in the presence of 1.33×10^{-2} mol kg^{-1} $OPPh_3$, 9.80×10^{-3} mol kg^{-1} PPh_3, and 1.62×10^{-3} mol kg^{-1} H_2O (B). The spectra were taken at 20 ns (a), 500 ns (b), and 20 μs (c) after a 355 nm laser irradiation.

Although the bell-shaped ligand concentration dependence of k_{obsd} is hardly seen for the slow process of the photoreaction of [Cr(OEP)(Cl)($OPPh_3$)] as shown in Figure 4B, it is probable that the axial substitution reaction of H_2O in [Cr(OEP)(Cl)(H_2O)] by $OPPh_3$ occurs by a mechanism similar to the case of [Cr(OEP)(Cl)(Py)]. We have analyzed the kinetic results for this slow process using an equation similar to eq 8 with a fixed value of k_{-H_2O} determined from the [Cr(OEP)(Cl)(Py)] and [Cr(OEP)(Cl)(H_2O)] systems mentioned above. The obtained kinetic and thermodynamic parameters listed in Table 1 explain the observed kinetic behavior shown by the solid lines in Figure 4B.

Photoreaction of [Cr(OEP)(Cl)($OPPh_3$)] in Dichloromethane Containing PPh_3. The absorption spectrum of the Cr(III)−OEP complex was measured in the presence of large excesses of $OPPh_3$ and PPh_3 over the porphyrin complex, and it was the same as that of [Cr(OEP)(Cl)($OPPh_3$)]. This is probably due to the stronger coordinating ability of $OPPh_3$ toward the chromium atom than PPh_3. In Figure 5, the transient absorbance difference spectra observed for the solution of the Cr(III)−OEP complex containing excess amounts of $OPPh_3$ and PPh_3 are shown. The transient spectrum observed at 20 ns after a laser irradiation is quite similar to that observed for the solution of [Cr(OEP)(Cl)($OPPh_3$)] just after laser irradiation (Figure 3a), indicating the formation of the five-coordinate complex, [Cr(OEP)(Cl)]. On the other hand, the second transient spectrum observed at 500 ns after a laser pulse is quite different from the second transient spectrum for the solution that does not contain PPh_3. A new positive absorption band was observed around 470

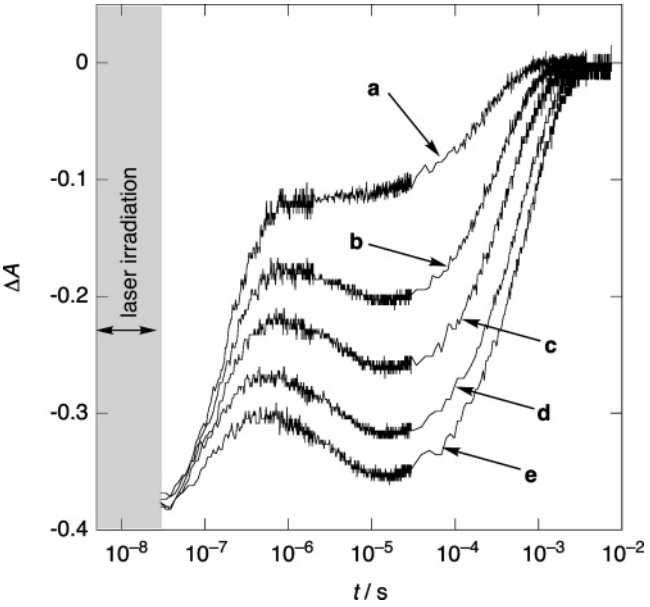

Figure 6. Absorbance−time traces of the photoreaction of the dichloromethane solution of [Cr(OEP)(Cl)($OPPh_3$)] in the presence of PPh_3. [$OPPh_3$] = 2.94×10^{-3} mol kg^{-1}, [H_2O] = $(2.0-2.2) \times 10^{-3}$ mol kg^{-1}, and [PPh_3]/mol kg^{-1} = 0 (a), 2.08×10^{-3} (b), 4.17×10^{-3} (c), 8.34×10^{-3} (d), and 1.11×10^{-2} (e). T = 25.0 °C.

nm as shown in Figure 5. Within 20 μs this second transient spectrum gradually changed to the third one, the shape of which is similar to that of the second transient spectrum. This spectral change depends on the conditions: the lower the concentration of $OPPh_3$, the larger the absorbance change for this process. Because the initial transient spectrum can be attributed to [Cr(OEP)(Cl)], the second and third transient spectra can be considered as an indication of the formation of the transient species [Cr(OEP)(Cl)(PPh_3)] and [Cr(OEP)(Cl)(H_2O)], and the concentration of these two transient species depends on the ligand concentrations. These species should be given by the reaction of photoinduced [Cr(OEP)(Cl)] and the bulk PPh_3 and H_2O molecules, respectively. The third transient spectrum decays back to the initial absorption spectrum in the time range of microseconds to milliseconds. The absorbance−time traces at the Soret band of [Cr(OEP)(Cl)($OPPh_3$)] are shown in Figure 6, and the three-step process of the decay of the transient spectrum, which we call the fast process, medium process, and slow process, is clearly shown.

As mentioned above, the fast process gives a mixture of the transient species [Cr(OEP)(Cl)(PPh_3)] and [Cr(OEP)(Cl)(H_2O)], and at the end of this process an equilibrium between these two transient species is not established due to the relatively slow rate of the reverse reactions. The amount of these intermediate complexes is proportional to the forward rate constant of the reaction of [Cr(OEP)(Cl)] with PPh_3 or H_2O, and the ratio of [Cr(OEP)(Cl)(H_2O)] over the total amount of these two transient species can be given by

$$R_1 = k_{H_2O}[H_2O](k_{PPh_3}[PPh_3] + k_{H_2O}[H_2O])^{-1} \quad (9)$$

The medium process and slow process can be ascribed to the processes of equilibration. Since the reaction of [Cr(OEP)(Cl)] with $OPPh_3$ to give the final product, [Cr(OEP)(Cl)($OPPh_3$)], is relatively slow, the medium process can be ascribed to the process of equilibration between [Cr(OEP)(Cl)(PPh_3)] and [Cr(OEP)(Cl)(H_2O)] produced through the fast process. In the time range of the medium process, the reverse reactions of the formation of these transient complexes are sufficiently fast, while the formation of the final product [Cr(OEP)(Cl)($OPPh_3$)] is too slow to participate. After establishing the equilibrium between [Cr(OEP)(Cl)(PPh_3)] and [Cr(OEP)(Cl)(H_2O)], a much slower reaction back to [Cr(OEP)(Cl)($OPPh_3$)] occurs in the microsecond to millisecond time frame (slow process). The reaction mechanism is shown in Scheme 1. According to the proposed mechanism, the ratio of [Cr(OEP)(Cl)(H_2O)] over the sum of [Cr(OEP)(Cl)(PPh_3)] and [Cr(OEP)(Cl)(H_2O)] after the medium process can be expressed by

$$R_2 = k_{-PPh_3}k_{H_2O}[H_2O](k_{-H_2O}k_{PPh_3}[PPh_3](1 + K_{(OPPh_3)}[OPPh_3])^{-1} + k_{-PPh_3}k_{H_2O}[H_2O])^{-1} \quad (10)$$

Values of R_1 and R_2 can be estimated by using rate constants (vide infra) for the experimental conditions of the transient spectrum measurements shown in Figure 5: R_1 = 0.40 and R_2 = 0.24 for Figure 5A; R_1 = 0.43 and R_2 = 0.41 for Figure 5B. These values are consistent with the spectral change of the medium process shown in Figure 5.

As in the case of the fast process of the photoreaction of the [Cr(OEP)(Cl)($OPPh_3$)] solution without PPh_3, the fast process of the present reaction system is the three parallel reversible reactions shown in Scheme 1. The absorbance−time traces are the sum of three exponential functions, and we did not analyze the reaction curves to determine the rate constants involved in these reactions. Instead, the kinetic parameters can be obtained from the medium process and slow process. The medium process corresponds to the equilibration of the transient species, [Cr(OEP)(Cl)(H_2O)] and [Cr(OEP)(Cl)(PPh_3)], produced through the fast process. The reaction is first-order with respect to the complex, and the dependence of k_{obsd} on the concentration of PPh_3 is shown in Figure 7A.[31] The mechanism of this process can be expressed as

$$[Cr(OEP)(Cl)(H_2O)] + OPPh_3 \overset{K_{(OPPh_3)}}{\rightleftharpoons} [Cr(OEP)(Cl)(HOH\cdots OPPh_3)] \quad (11)$$

$$[Cr(OEP)(Cl)(H_2O)] \underset{k_{H_2O}}{\overset{k_{-H_2O}}{\rightleftharpoons}} [Cr(OEP)(Cl)] + H_2O \quad (12)$$

$$[Cr(OEP)(Cl)] + PPh_3 \underset{k_{-PPh_3}}{\overset{k_{PPh_3}}{\rightleftharpoons}} [Cr(OEP)(Cl)(PPh_3)] \quad (13)$$

By applying the steady-state approximation with respect to the five-coordinate intermediate [Cr(OEP)(Cl)], the pseudo-first-order rate constant is expressed as

$$k_{obsd} = (k_{-H_2O}k_{PPh_3}[PPh_3](1 + K_{(OPPh_3)}[OPPh_3])^{-1} + k_{-PPh_3}k_{H_2O}[H_2O])(k_{PPh_3}[PPh_3] + k_{H_2O}[H_2O])^{-1} \quad (14)$$

The least-squares analysis of the data shown in Figure 7A

Scheme 1

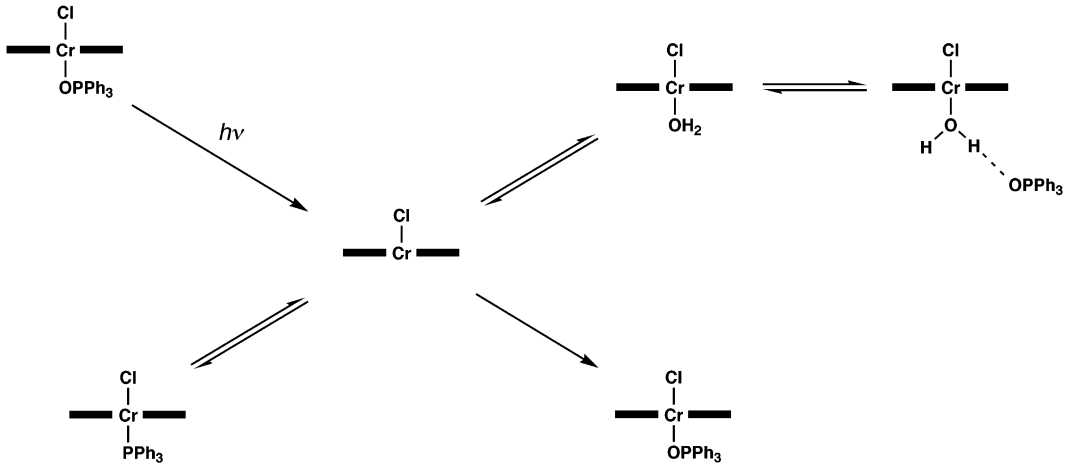

based on eq 14 was done together with the kinetic results for the slow process because these two processes include identical elementary processes of ligand-binding and ligand-dissociation reactions (vide supra).

Once the equilibrium between [Cr(OEP)(Cl)(H_2O)] and [Cr(OEP)(Cl)(PPh_3)] is established through the medium process, then the slower, succeeding reaction (slow process) occurs, as shown in Figure 6. k_{obsd} depends on the concentration of H_2O and $OPPh_3$ of the bulk solution in the same manner as the slow process of the photoreaction of [Cr(OEP)-(Cl)($OPPh_3$)], and k_{obsd} also depends on the concentration of PPh_3, as shown in Figure 7B. As the concentration of PPh_3 increases, k_{obsd} decreases. Based on the mechanism shown in Scheme 1, the pseudo-first-order rate constant is expressed by eq 15 by applying the steady-state approximation to the five-coordinate intermediate [Cr(OEP)(Cl)].

$$k_{obsd} = (k_{-H_2O}k_{OPPh_3}[OPPh_3](1 + k_{PPh_3}[PPh_3]k_{H_2O}{}^{-1}[H_2O]^{-1}))(k_{H_2O}[H_2O] + k_{PPh_3}[PPh_3] + k_{OPPh_3}[OPPh_3])^{-1}(1 + K_{(OPPh_3)}[OPPh_3] + k_{-H_2O}k_{PPh_3}k_{H_2O}{}^{-1}k_{-PPh_3}{}^{-1}[PPh_3][H_2O]^{-1})^{-1} \quad (15)$$

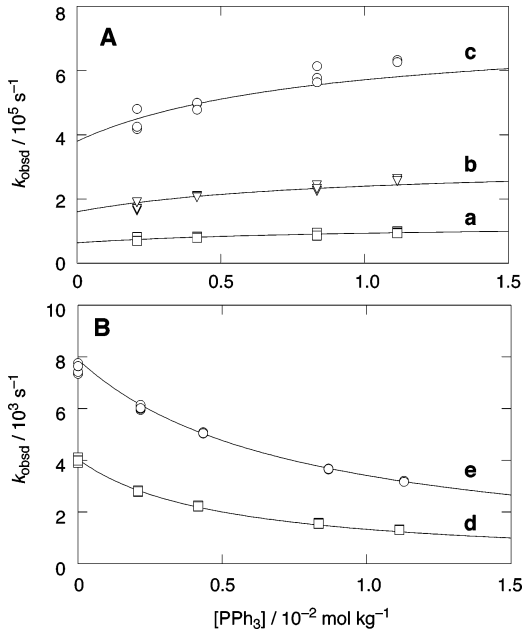

Figure 7. Plot of the pseudo-first-order rate constant k_{obsd} of the medium process (A) and the slow process (B) of the photoreaction of the dichloromethane solution of [Cr(OEP)(Cl)($OPPh_3$)] in the presence of PPh_3 as a function of the concentration of PPh_3. A: [$OPPh_3$] = 2.94×10^{-3} mol kg^{-1}, [H_2O] = $(2.0-2.2) \times 10^{-3}$ mol kg^{-1}. T = 15.0 (a), 25.0 (b), and 35.0 °C (c). B: [$OPPh_3$]/mol kg^{-1} = 2.94×10^{-3} (d) and 8.91×10^{-3} (e). [H_2O] = $(2.0-2.2) \times 10^{-3}$ mol kg^{-1}. T = 25.0 °C.

The least-squares analysis for the kinetic results of the medium process and slow process, as shown in Figure 7, was done simultaneously to determine the kinetic parameters k_{PPh_3} and k_{-PPh_3} using values of other rate constants and $K_{(OPPh_3)}$ evaluated from the photoreaction of [Cr(OEP)(Cl)(H_2O)] and [Cr(OEP)(Cl)($OPPh_3$)]. Obtained values of the kinetic parameters are listed in Table 1.

Quantum Yield Measurements. The quantum yield, Φ_{diss}, for the photodissociation of the axial ligand L (L = H_2O, Py, and $OPPh_3$) from [Cr(OEP)(Cl)(L)] in dichloromethane was determined by laser flash photolysis. In the present study, the laser irradiation of [Cr(OEP)(Cl)(L)] gives solely the five-coordinate species, [Cr(OEP)(Cl)], immediately after the laser pulse, and the formation of the triplet excited states could not be detected. Φ_{diss} is expressed as

$$\Phi_{diss} = \Delta A_{diss}\Delta\epsilon_1{}^{-1}I_{abs}{}^{-1}N_A \quad (16)$$

where ΔA_{diss}, $\Delta\epsilon_1$, I_{abs}, and N_A represent the absorbance change just after the laser excitation at a monitoring wavelength, the difference in the molar absorption coefficients between [Cr(OEP)(Cl)] and [Cr(OEP)(Cl)(L)], the number of photons absorbed by [Cr(OEP)(Cl)(L)], and Avogadro's number, respectively. The molar absorption coefficient of the five-coordinate intermediate [Cr(OEP)(Cl)] was determined by the method previously described.[18] Figure

(31) It is difficult to study the dependence of k_{obsd} of the medium process on the concentration of $OPPh_3$ because the absorbance change becomes smaller when the concentration of $OPPh_3$ becomes larger. Judging from the mechanism of the slow process of the corresponding reaction system, it is probable that the preequilibrium (eq 11) may participate in the medium process of the photoreaction.

S4 (Supporting Information) shows the absorption spectrum of [Cr(OEP)(Cl)] as well as that of [Cr(OEP)(Cl)(L)] (L = H_2O and Py). To estimate the I_{abs} value, a benzene solution of zinc(II) tetraphenylporphyrin, [Zn(TPP)], which has the same absorbance at the laser excitation wavelength (532 nm) as that of the dichloromethane solution of [Cr(OEP)(Cl)(L)], was used as a reference for the quantum yield measurements. When the benzene solution of [Zn(TPP)] is subjected to the laser pulse, the triplet excited state of [Zn(TPP)], which has an absorption band around the 470 nm region, is produced. The absorbance change, ΔA_T, at 470 nm after the laser pulse is expressed as

$$\Delta A_T = \Phi_T \epsilon_T I_{abs} N_A^{-1} \quad (17)$$

where Φ_T (0.83) and ϵ_T (7.3×10^4 M^{-1} cm^{-1}) are the triplet yield of [Zn(TPP)] and the molar absorption coefficient of the triplet excited state of [Zn(TPP)] at 470 nm, respectively.[32] From eqs 16 and 17, eq 18 is derived:

$$\Phi_{diss} = \Delta A_{diss} \Delta A_T^{-1} \epsilon_T \Delta \epsilon_1^{-1} \Phi_T \quad (18)$$

The values of Φ_{diss} were determined as 0.64 ± 0.03 (L = H_2O), 0.76 ± 0.03 (L = Py), and 0.64 ± 0.03 (L = $OPPh_3$). The effect of dioxygen on Φ_{diss} was investigated under the conditions of P_{O2} = 0−1 atm, and it was revealed that dioxygen has no effect on the quantum yield of the photodissociation of L (L = H_2O, Py, and $OPPh_3$) from [Cr(OEP)(Cl)(L)].

Axial Substitution Reaction of [Cr(OEP)(Cl)($OPPh_3$)] by Py. Laser photolysis provides kinetic parameters for the dissociation of L from [Cr(OEP)(Cl)(L)] and those for the binding of L to the five-coordinate complex, [Cr(OEP)(Cl)], as mentioned above (L = H_2O, PPh_3). However, the kinetic parameters for the axial $OPPh_3$ dissociation reaction from [Cr(OEP)(Cl)($OPPh_3$)] were not obtained from these experiments since the rate of this reaction is too slow to participate in the photoreaction dynamics. To determine these kinetic parameters, we studied the kinetics of the axial substitution reaction of [Cr(OEP)(Cl)($OPPh_3$)] by Py in dichloromethane using a stopped-flow apparatus. A dichloromethane solution of [Cr(OEP)(Cl)($OPPh_3$)] containing an excess amount of $OPPh_3$ was mixed with the Py solution, and the progress of the substitution reaction was monitored spectrophotometrically. The spectrum of the initial $OPPh_3$ complex was converted to that of the Py complex with well-defined isosbestic points. The overall reaction can be expressed by eq 19.

$$[Cr(OEP)(Cl)(OPPh_3)] + Py \rightleftharpoons [Cr(OEP)(Cl)(Py)] + OPPh_3 \quad (19)$$

The reaction rates were measured under various conditions where entering and leaving ligands were present in large excess over the porphyrin complex. The reaction was first-order with respect to the porphyrin complex. k_{obsd} was plotted against the ratio of the concentration of entering and leaving ligands in the bulk solution, as shown in Figure S5 (Supporting Information). At a constant concentration of $OPPh_3$, the rate constant first decreases with an increase in the Py concentration and finally converges to a constant value at a higher Py concentration, while the rate increases with an increase in the concentration of $OPPh_3$ at a constant Py concentration. These results can be interpreted by a dissociative mechanism, as shown in eqs 20 and 21.

$$[Cr(OEP)(Cl)(OPPh_3)] \underset{k_{OPPh_3}}{\overset{k_{-OPPh_3}}{\rightleftharpoons}} [Cr(OEP)(Cl)] + OPPh_3 \quad (20)$$

$$[Cr(OEP)(Cl)] + Py \underset{k_{-Py}}{\overset{k_{Py}}{\rightleftharpoons}} [Cr(OEP)(Cl)(Py)] \quad (21)$$

By applying the steady-state approximation to [Cr(OEP)(Cl)], the pseudo-first-order rate constant can be given by

$$k_{obsd} = (k_{-OPPh_3}[Py] + k_{OPPh_3} k_{Py}^{-1} k_{-Py}[OPPh_3])(k_{OPPh_3} k_{Py}^{-1}[OPPh_3] + [Py])^{-1} \quad (22)$$

The values of k_{-OPPh_3}, $k_{OPPh_3}k_{Py}^{-1}$, and k_{-Py} at each temperature were determined by applying the least-squares fitting calculation to the ligand concentration dependence of k_{obsd}. Since the Eyring's plots of k_{-OPPh_3}, $k_{OPPh_3}k_{Py}^{-1}$, and k_{-Py} proved linear within experimental error, the enthalpy and entropy of activation were determined by simultaneously fitting the variable-temperature data to eq 22 and the Eyring equation. Kinetic parameters thus obtained are summarized in Table 2.

Table 2. Kinetic Parameters[a] for the Axial Substitution Reaction of [Cr(OEP)(Cl)($OPPh_3$)] by Pyridine at T = 25.0 °C [b]

k_{-OPPh_3} (s^{-1})	2.48
$\Delta H_{-OPPh_3}^{\ddagger}$	77.8 ± 0.7
$\Delta S_{-OPPh_3}^{\ddagger}$	23.5 ± 2.3
k_{-Py} (s^{-1})	6.56
$\Delta H_{-Py}^{\ddagger}$	89.1 ± 1.9
$\Delta S_{-Py}^{\ddagger}$	69.4 ± 6.4
k_{OPPh_3}/k_{Py}	1.57×10^{-2}
$\Delta H_{OPPh_3}^{\ddagger} - \Delta H_{Py}^{\ddagger}$	8.4 ± 4.0
$\Delta S_{OPPh_3}^{\ddagger} - \Delta S_{Py}^{\ddagger}$	−6 ± 13

[a] ΔH, kJ mol^{-1}; ΔS, J mol^{-1} K^{-1}. [b] Values of the rate and equilibrium constants were calculated by using the determined $\Delta H^{\ddagger}$, $\Delta S^{\ddagger}$, $\Delta H°$, and $\Delta S°$.

Molecular Structure of [Cr(TPP)(Cl)($OPPh_3$)]. In the present study, we investigated the photochemical reaction of the Cr−OEP complexes in solution. To obtain supporting evidence about the dynamic properties of the complexes involved in the steric effect caused by the bulky PPh_3 ligand, we tried to prepare a single crystal of the Cr−OEP complex having an axial PPh_3 ligand and related complexes, but an X-ray-quality single crystal was not obtained. Instead, we succeeded in preparing a single crystal of [Cr(TPP)(Cl)($OPPh_3$)]. The molecular structure of [Cr(TPP)(Cl)($OPPh_3$)] is shown in Figure 8. Crystallographic data are listed in Table 3. The selected bond lengths and angles are listed in Table 4. The four equatorial Cr−N lengths (2.027(4), 2.030(4), 2.028(4), and 2.033(4) Å) are close to each other. The average Cr−N bond length of 2.030 Å is almost the same as those of other Cr(III) porphyrins.[17,18,22] The axial Cr−Cl

(32) Hurley, J. K.; Sinai, N.; Linschitz, H. *Photochem. Photobiol.* **1983**, *38*, 9−14.

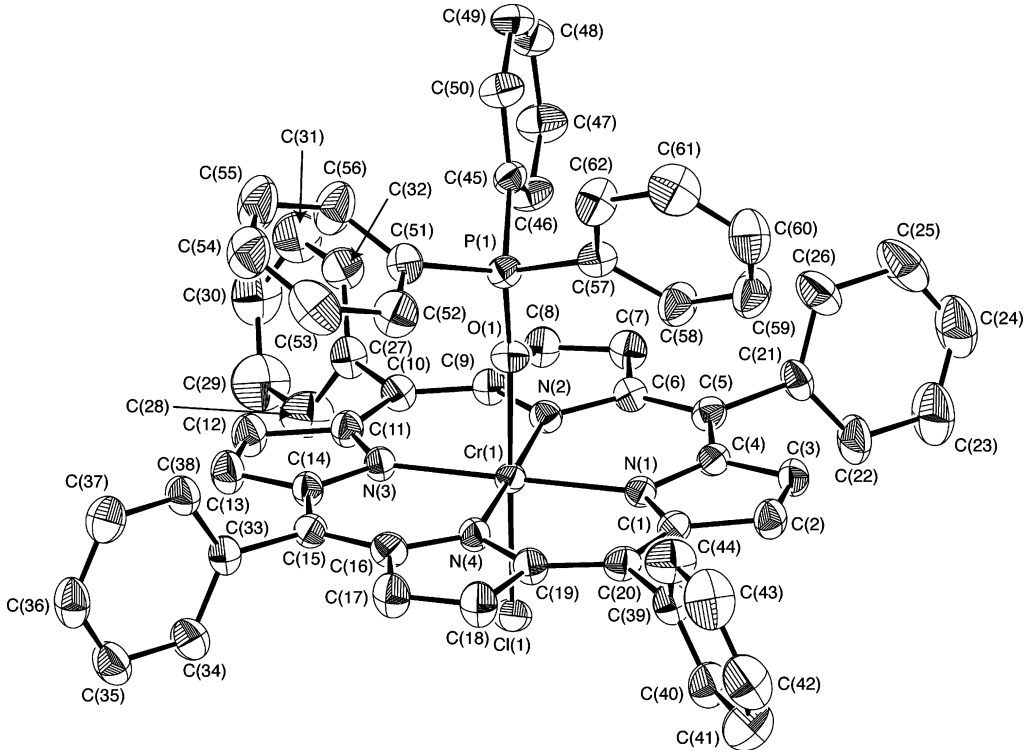

Figure 8. Molecular structure of [Cr(TPP)(Cl)($OPPh_3$)].

Table 3. Crystallographic Data and Experimental Details

compound	[Cr(TPP)(Cl)($OPPh_3$)]·0.5C_7H_8·0.5$C_2H_4Cl_2$·H_2O
formula	$C_{66.5}H_{51}N_4O_2PCl_2Cr$
M	1092.05
cryst syst	monoclinic
space group	$P2_1/n$
a (Å)	24.8385(4)
b (Å)	17.9520(4)
c (Å)	13.3714(2)
α (deg)	90
β (deg)	89.699(2)
γ (deg)	90
Z	4
V (Å^3)	5962.2(2)
μ(Mo Kα) (cm^{-1})	3.03
transm factor	0.9083−0.9644
cryst size (mm^3)	0.18 × 0.24 × 0.50
d_{calcd} (g cm^{-3})	1.092
λ(Mo Kα) (Å)	0.710 69
T (°C)	25
$2\theta_{max}$ (deg)	55
R [a]	0.0838
R_w [b]	0.1174

[a] $R = \Sigma||F_o| - |F_c||/\Sigma|F_o|$. [b] $R_w = [\Sigma w(|F_o| - |F_c|)^2/\Sigma w|F_o|^2]^{1/2}$; $w = [\sigma_c^2(F_o) + (p^2/4)|F_o|^2]^{-1}$; $p = 0.0700$.

Table 4. Selected Bond Lengths (Å) and Angles (deg) of the Porphyrin Complex

Cr(1)−Cl(1)	2.300(2)	Cr(1)−N(3)	2.028(4)
Cr(1)−O(1)	2.033(4)	Cr(1)−N(4)	2.033(4)
Cr(1)−N(1)	2.027(4)	P(1)−O(1)	1.489(4)
Cr(1)−N(2)	2.030(4)		
Cl(1)−Cr(1)−O(1)	179.1(1)	O(1)−Cr(1)−N(4)	89.4(2)
Cl(1)−Cr(1)−N(1)	90.7(1)	N(1)−Cr(1)−N(2)	90.5(2)
Cl(1)−Cr(1)−N(2)	91.1(1)	N(1)−Cr(1)−N(3)	179.4(2)
Cl(1)−Cr(1)−N(3)	89.8(1)	N(1)−Cr(1)−N(4)	89.6(2)
Cl(1)−Cr(1)−N(4)	91.4(1)	N(2)−Cr(1)−N(3)	89.8(2)
O(1)−Cr(1)−N(1)	88.8(2)	N(2)−Cr(1)−N(4)	177.5(2)
O(1)−Cr(1)−N(2)	88.1(1)	N(3)−Cr(1)−N(4)	90.1(2)
O(1)−Cr(1)−N(3)	90.6(2)	Cr(1)−O(1)−P(1)	174.0(2)

bond length of 2.300(2) Å is close to that of the related complexes, i.e., [Cr(TPP)(Cl)(Py)] (2.311(2) Å),[18] [Cr(TPP)(Cl)(1-MeIm)] (2.317(2) Å, 1-MeIm = 1-methylimidazole),[17] [Cr(TPP)(Cl)(1,2-Me_2Im)] (2.315(2) Å, 1,2-Me_2Im = 1,2-dimethylimidazole),[17] and [Cr(TPP)(Cl)(H_2O)](2-MePy)$_2$ (2.3114(7) Å, 2-MePy = 2-methylpyridine).[22] The axial Cr−O bond length is 2.033(4) Å, which is also close to the distance between Cr and the oxygen atom of the axial H_2O ligand in [Cr(TPP)(Cl)(H_2O)](2-MePy)$_2$ (2.057(2) Å).[22] Figure S6 (Supporting Information) shows the perpendicular displacements of the atoms from the mean plane of the respective 24-atom porphyrin core. The root mean square (rms) displacement for the entire core is 0.034 Å. The chromium atom is located 0.043(1) Å from the mean plane of the porphyrin core toward the chlorine atom. The Cl−Cr−O angle of 179.1(1)° and the N−Cr−O angles which span the range 89.8(1)−91.4(1)° are consistent with an in-plane arrangement of the central chromium atom. The Cr−O−P angle of 174.0(2)° is larger than the corresponding value of 154.2(5)° for [Os(OEP)($OPPh_3$)$_2$],[33] but it is still within the range of the metal−O−P angles in $OPPh_3$ complexes of around 140−180°.

Discussion

It has been well-recognized that the excited singlet and triplet states of the porphyrin π system of the chromium(III) porphyrin complex weakly interact with the central chromium atom ($S = 3/2$), giving singquartet ($^4S_1$), tripdoublet ($^2T_1$), tripquartet ($^4T_1$), and tripsextet ($^6T_1$) excited states.[34,35] The lowest and second-lowest excited states, $^6T_1$

(33) Che, C.-M.; Lai, T.-F.; Chung, W.-C.; Schaefer, W. P.; Gray, H. B. *Inorg. Chem.* **1987**, *26*, 3907−3911.

Table 5. Kinetic and Thermodynamic Parameters for the Reaction of [Cr(OEP)(Cl)] with L at $T = 25.0$ °C

	k_L (mol^{-1} $kg\ s^{-1}$)	k_{-L} (s^{-1})	K_L [a] (mol^{-1} kg)	$\Delta H_L°$ (kJ mol^{-1})	$\Delta S_L°$ (J mol^{-1} K^{-1})
H_2O	2.45×10^9	4.17×10^5	5.9×10^3	−50	−95
Py	1.51×10^9	6.56	2.3×10^8	−82	−116
$OPPh_3$	2.33×10^7	2.48	9.4×10^6	−61	−70
PPh_3	5.53×10^8	1.61×10^5	3.4×10^3	−51	−102

[a] The value of the equilibrium constant K_L was estimated using the relationship $K_L = k_L k_{-L}^{-1}$.

and $^4T_1$, are in thermal equilibrium. We previously reported on the photochemistry of the chromium(III) porphyrin complexes with various axial ligands in order to clarify the mechanism of photophysical and photochemical processes, including the axial ligand dissociation and recombination reactions.[18−23] Laser photolysis studies have revealed that photoinduced physical and chemical processes depend on the nature of the porphyrin ligand and the chemical bond between the chromium atom and the axial ligand, as well as the reaction medium. Based on the quantum yield measurements, it was found that the photoelimination of the axial ligand occurs via two reaction paths, i.e., those through the $^4S_1$ and $^6T_1$ excited states, and that the yield of the photoelimination largely depends on the donor ability of the axial ligand. As for the tetraphenylporphyrin complex, [Cr(TPP)(Cl)(Py)], the quantum yield of the axial Py dissociation in the toluene solution is 0.65, in which the quantum yield of 0.18 and 0.47 is through the singlet and triplet excited states, respectively.[21] The corresponding quantum yield for the OEP complex, [Cr(OEP)(Cl)(Py)], in toluene is 0.89, which was solely attributed to the singlet excited state.[23] The difference in the quantum yield of these two complexes can be attributed to the nature of the porphyrin ligand. For the OEP complex, the axial ligand dissociation through the triplet excited state can only be observed when the complex has a stronger chemical bond at an axial site such as [Cr(OEP)(Cl)(1-MeIm)]. In the present study, based on the independence of the quantum yield on the dioxygen concentration, it was revealed that the photodissociation reactions occur at the singlet excited state for all complexes investigated here. Participation of the triplet excited state in the photodissociation of the axial ligand depends on the efficiency of the intersystem crossing from $^4S_1$ to $^4T_1$ competing with the dissociation of the axial ligand at the $^4S_1$ state. Therefore, it can be concluded that the chemical bond between the chromium atom and the axial ligand L in [Cr(OEP)(Cl)(L)] is not so strong even for L = $OPPh_3$ that the intersystem crossing from $^4S_1$ to $^4T_1$ could not be observed due to the facile axial ligand dissociation at the $^4S_1$ state.

In the present study, the rate constants of the dissociation reaction of the axial ligand L from [Cr(OEP)(Cl)(L)] (L = H_2O, Py, PPh_3, and $OPPh_3$) at the electronic ground state and those of the ligand association to [Cr(OEP)(Cl)] were determined as listed in Table 5. The ligand association rate constant, k_L, is extremely large, and the difference in these activation parameters is not very large, indicating that the reactivity of the five-coordinate intermediate toward the ligand association reaction is so high that the discriminating ability of the intermediate toward the entering ligand is poor. These findings are in accord with a small activation enthalpy and negative activation entropy for the axial ligand binding reaction. The energy required for orientation of the reacting molecules in a favorable configuration may be small for the present reaction, like other metalloporphyrins with very large rate constants (in the range of 10^8-10^9 mol^{-1} kg s^{-1}) for the axial ligand rebinding for Fe(II)[36−38] and Co(III)[39−41] porphyrins.

Even though the k_L value is extremely large for all ligands, as mentioned above, its value is somewhat smaller for the ligand that suffers from the steric hindrance caused by the substituents around the donor atom of the ligand during the complexation reaction with [Cr(OEP)(Cl)]: a large entering ligand such as PPh_3 may not favor the bimolecular reaction due to the low probability of a relative geometrical arrangement of the colliding molecules, and in addition, the activation enthalpy for PPh_3 is higher than that of H_2O by about 5 kJ mol^{-1}, which implies that [Cr(OEP)(Cl)] prefers H_2O to PPh_3 energetically. It is noteworthy that the most crowded PPh_3 ligand shows higher reactivity than the less crowded $OPPh_3$ ligand, probably due to the higher nucleophilicity of PPh_3. A similar association reaction of PPh_3 with coordinately unsaturated metalloporphyrins has been investigated using laser flash photolysis, and the observed value of k_L was 6.9×10^7 M^{-1} s^{-1} (25 °C) for [Rh(OEP)(I)],[42] which is slightly smaller than that of the present complex.

In contrast to the relatively small difference in the reactivity of the ligand association reaction to [Cr(OEP)(Cl)], the rate constant of the dissociation of the ligand L from [Cr(OEP)(Cl)(L)] extends over 5 orders of magnitude, and the difference in the activation enthalpy amounts to more than 30 kJ mol^{-1}. Such features in activation parameters can be considered an indication that the bond between the chromium atom and the donor atom of the axial ligand L is almost broken at the transition state of the axial ligand dissociation reaction, reflecting the reaction mechanism of the present ligand substitution process. The difference in the rate constant of the axial ligand dissociation reaction between the PPh_3 and $OPPh_3$ complexes, which amounts to a factor of 6×10^4, should reflect the intrinsic properties of the chemical bond at the axial coordination site of the complex. The more labile character of PPh_3 should reflect the

(34) Gouterman, M.; Hanson, L. K.; Khalil, G.-E.; Leenstra, W. R.; Buchler, J. W. *J. Chem. Phys.* **1975**, *62*, 2343−2353.
(35) Harriman, A. *J. Chem. Soc., Faraday Trans. 1* **1982**, *78*, 2727−2734.
(36) Lavalette, D.; Tetreau, C.; Momenteau, M. *J. Am. Chem. Soc.* **1979**, *101*, 5395−5401.
(37) Dixon, D. W.; Kirmaier, C.; Holten, D. *J. Am. Chem. Soc.* **1985**, *107*, 808−813.
(38) Maillard, P.; Schaeffer, C.; Tétreau, C.; Lavalette, D.; Lhoste, J.-M.; Momenteau, M. *J. Chem. Soc., Perkin Trans. 2* **1989**, 1437−1442.
(39) Tait, C. D.; Holten, D.; Gouterman, M. *Chem. Phys. Lett.* **1983**, *100*, 268−272.
(40) Tait, C. D.; Holten, D.; Gouterman, M. *J. Am. Chem. Soc.* **1984**, *106*, 6653−6659.
(41) Hoshino, M.; Kogure, M.; Asano, K.; Hinohara, T. *J. Phys. Chem.* **1989**, *93*, 6655−6659.
(42) Suzuki, H.; Miyazaki, Y.; Hoshino, M. *J. Phys. Chem. A* **2003**, *107*, 1239−1245.

intrinsically less attractive interaction of the phosphorus ligand with the chromium(III) ion compared with the oxygen ligand. In addition to this, the steric interaction caused by the steric bulk of the axial ligand may affect the dynamics of the axial ligand dissociation reaction. Although we were unable to obtain an X-ray-quality single crystal of the PPh_3 complexes in the present study, it is expected that the steric bulk of the PPh_3 ligand might cause the repulsive interaction with the porphyrin ligand due to the smaller distance between the phenyl group of PPh_3 and the porphyrin π electron system. Evidence of such interactions can be seen in an umbrella-like conformation of the porphyrin core with the pyrrole β-carbon atoms of OEP bowed toward the axial Cl ligand trans to PPh_3 observed in [Rh(OEP)(Cl)(PPh_3)].[43] This type of deformation of the porphyrin core can also be demonstrated in the tetraphenylpoprhyin complex having a related phosphine ligand, diphenyl(phenylacetenyl)phosphine, in [Rh(TPP)(CH_3)(L)] (L = diphenyl(phenylacetenyl)phosphine).[44] The peripheral phenyl substituents of tetraphenylporphyrin are also bowed toward the axial methyl group to minimize steric interactions between the phosphine ligand and the phenyl substituents of the porphyrin. Similar steric interactions can be expected for [Cr(OEP)(Cl)(PPh_3)] since the bond length between the Cr and P atoms should be shorter than that between the Rh and P atoms. On the other hand, [Cr(TPP)(Cl)($OPPh_3$)] shows a relatively planar porphyrin skeleton, which is documented in Figure S6 (Supporting Information). The individual atomic displacements for the porphyrin skeleton are all <0.08 Å, indicating that the steric interaction between the porphyrin ligand and the axial Cl and $OPPh_3$ ligands can be negligible. Since the steric bulk of the peripheral substituents is less pronounced for OEP than TPP, repulsive interaction due to the $OPPh_3$ ligand is also negligible for [Cr(OEP)(Cl)($OPPh_3$)]. Therefore, the expected repulsive interaction between the porphyrin skeleton and the PPh_3 ligand in [Cr(OEP)(Cl)(PPh_3)] should cause the weakening of the axial bond and be partly reflected in the more labile nature of the axial PPh_3 ligand compared with the $OPPh_3$ complex.

As has been suggested from the UV−visible absorption spectrum shown in Figure 1, $OPPh_3$ should show a higher affinity for coordination to the central chromium atom of the OEP complex than PPh_3, and this can be rationalized by the equilibrium constant of the reaction of the five-coordinate [Cr(OEP)(Cl)] with ligand L, as listed in Table 5. The equilibrium constant for $OPPh_3$ is 3000 times larger that that of PPh_3. When PPh_3 is possibly contaminated with its oxidation product, $OPPh_3$, even in a quantity as small as 0.1%, the spectrum of the solution containing the Cr(III)−OEP complex and PPh_3 should exhibit an absorption spectrum similar to that of [Cr(OEP)(Cl)($OPPh_3$)] as demonstrated in Figure 1. Such a difference in the equilibrium constant is caused by the much smaller k_{-L} value of the $OPPh_3$ complex as compared with the PPh_3 complex even though the k_L value of $OPPh_3$ is 1/20th of that of PPh_3.

Conclusion

Photoreactions of the chromium(III) octaethylpoprhyrin complex, [Cr(OEP)(Cl)(L)] (L = H_2O, Py, $OPPh_3$), in dichloromethane were studied using a nanosecond laser flash photolysis technique. The laser irradiation causes efficient axial ligand dissociation at the electronic excited state of the complex, probably at the $^4S_1$ state, to produce a five-coordinate intermediate, [Cr(OEP)(Cl)], and the generation of the triplet excited states was not observed. The reactivity of [Cr(OEP)(Cl)] toward external ligands in the solution is extremely high, and the transient complex [Cr(OEP)(Cl)(H_2O)] can easily be produced through the reaction with the H_2O molecule in the dichloromethane solution when L = Py and $OPPh_3$. Transient spectra show that the axial H_2O ligand is then replaced by a ligand such as Py or $OPPh_3$ to regenerate the parent complex. Unfavorable coordination of the PPh_3 ligand to [Cr(OEP)(Cl)] was observed during the photoreaction of the [Cr(OEP)(Cl)($OPPh_3$)] solution containing an excess amount of PPh_3 in the bulk solution. Although the steric repulsion between the bulky PPh_3 ligand and the porphyrin skeleton is expected during the formation of [Cr(OEP)(Cl)(PPh_3)], the larger rate constant of the PPh_3 binding reaction compared with that for $OPPh_3$ results in the formation of [Cr(OEP)(Cl)(PPh_3)], which is eventually transformed to the parent complex, [Cr(OEP)(Cl)($OPPh_3$)], through the axial substitution reaction. Based on the rate law and the kinetic parameters of the reaction, a limited dissociative mechanism, including [Cr(OEP)(Cl)] as an intermediate, is ascribed to the photoinduced axial ligand substitution reactions of [Cr(OEP)(Cl)(L)] in solution.

Acknowledgment. This work was supported by a Grant-in-Aid for Scientific Research (No. 16550053 and No. 17550056) from the Ministry of Education, Science, Sports, and Culture of Japan.

Supporting Information Available: Figures reporting the kinetic results on the photoreaction of [Cr(OEP)(Cl)(H_2O)], the comparison of the transient spectrum of [Cr(OEP)(Cl)($OPPh_3$)] with the difference spectrum between [Cr(OEP)(Cl)(H_2O)] and [Cr(OEP)(Cl)($OPPh_3$)], the transient spectrum of [Cr(OEP)(Cl)(Py)], the UV−visible absorption spectrum of the five-coordinate [Cr(OEP)(Cl)], the kinetic results on the substitution reaction of [Cr(OEP)(Cl)($OPPh_3$)], a formal diagram of the porphyrin core, top and side views of the complex, tables reporting bond distances, angles, and positional and thermal parameters for the structurally characterized porphyrin complex, and one X-ray crystallographic file (in CIF format). This material is available free of charge via the Internet at http://pubs.acs.org.

IC0504487

(43) Thackray, D. C.; Ariel, S.; Leung, T. W.; Menon, K.; James, B. R.; Trotter, J. *Can. J. Chem.* **1986**, *64*, 2440−2446.
(44) Stulz, E.; Scott, S. M.; Bond, A. D.; Otto, S.; Sanders, J. K. M. *Inorg. Chem.* **2003**, *42*, 3086−3096.